www.cadanda.com
Computer-Aided Design AND APPLICATIONS

Design of a Micro Vertical Axis Wind Turbine: Modeling and Analysis

Mohammad U. A. Bhati[1] , Satchit Ramnath[2] , John Wagner[3]

[1]Department of Mechanical Engineering, Clemson University, mbhati@g.clemson.edu
[2]Department of Mechanical Engineering, Clemson University, sramnat@clemson.edu
[3]Department of Mechanical Engineering, Clemson University, jwagner@clemson.edu

Corresponding author: Satchit Ramnath, sramnat@clemson.edu

Abstract. Micro-sized wind turbines have the potential to generate electric power to charge portable or hand-held devices using wind. These lightweight renewable energy systems are portable and can quickly be deployed in remote locations like the ones encountered when hiking or camping. This paper investigates the aerodynamics and performance of eight different blade profiles chosen as possible candidates for a micro-vertical axis wind turbine. Commercial computational fluid dynamics packages were applied to calculate the blades' lift and drag coefficients. The numerical results for a typical low Reynolds Number of 77,000 showed that different blade profiles (e.g., *NACA 6409 9%, FX-77-121, Berget BW-3*) and parameters (e.g., camber radius, chord length) had a significant influence on the lift and drag coefficients. Overall, the combination-type blade designs offered the best performance, namely the Urginsky blade (using both C_L and C_D).

Keywords: wind turbine, vertical axis turbine, micro turbine, turbine design, blade design
DOI: https://doi.org/10.14733/cadaps.2026.340-357

1 INTRODUCTION

With global population growth, energy demand worldwide has skyrocketed to power industrial equipment and consumer goods. According to the U.S. Energy Information Administration (EIA), the world's energy consumption will increase in the year 2050 by 63.56 billion kWh (216.9 quadrillion BTUs) [29, 8]. Researchers have explored alternative energy sources and electric generation methods to meet this demand. The emphasis on green power, primarily from solar, wind, and hydropower, has gained the greatest attention, given their inherent sustainability and abundance. Solar energy, harnessed from the sun's radiant rays, offers a clean and limitless power source. Wind energy, captured from the kinetic energy of moving air, provides a versatile and scalable energy option. Hydropower, generated from water movement, has long been a reliable and renewable energy source. The transition towards a greener energy future is not without its challenges. Integrating renewable energy sources into existing power grids requires sophisticated grid management systems and energy

storage solutions. Additionally, the large-scale deployment of renewable energy infrastructure often faces regulatory hurdles and financial constraints. Despite these obstacles, pursuing a sustainable energy future remains an urgent and compelling endeavor. The potential benefits of renewable energy sources are undeniable, offering a path towards cleaner air, reduced greenhouse gas emissions, and a more secure energy supply for future generations. The ability to harness wind energy worldwide using portable turbines is a promising technology, especially given the relevance of consumer electronics.

The harnessing of wind energy is studied to meet the world's demand to power portable electronic devices with moderate charging requirements. Surface wind currents are generated by weather patterns, that establish regional temperatures, and the earth's rotation. The progression of wind energy over the past 2000 years has been illustrated in Figure 1. Modern wind turbines are primarily Horizontal Axis Wind Turbines (HAWT) which feature tall towers with three large fiberglass blades. The low-speed shaft driving the rotor enters the multiple planetary geared transmission so that the output high-speed shaft can turn the AC generator to produce electric power. On the other hand, Vertical Axis Wind Turbines (VAWT) have not received as much attention, but advantages exist for selecting VAWT over HAWT, especially in urban areas. VAWTs are omnidirectional, meaning they can receive wind from any direction, they are quieter than HAWTs, and the equipment has a smaller form factor than HAWTs, making them easier to set up and requiring less maintenance [13].

The availability of portable miniature wind turbines for the off-grid charging of personal devices remains an unfilled niche. Ideally, these lightweight generators can be quickly deployed in a variety of scenarios for power generation by harvesting available low-speed winds. The research presented features aerodynamic blade modeling and optimization, complemented with extensive analytical studies. The research seeks to develop optimum compact energy harvesting machines for both novice and experienced backpackers traveling through remote areas to charge critical electronics (e.g., satellite phones, medical sensors, etc.).

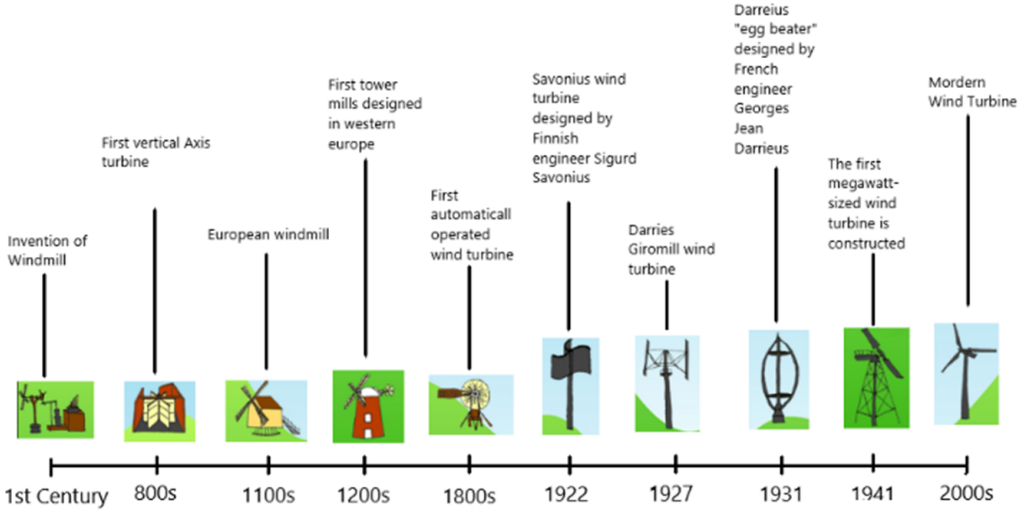

Figure 1: Illustration of wind energy harvesting technology over the past two thousand years

2 LITERATURE REVIEW

The open literature on vertical-axis wind turbines is small compared to other renewable energy solutions. Johari et al. [13] compared the performance of HAWTs and VAWTs under different wind speeds and behaviors. Their study aimed to encourage wind power generation in Malaysia's windy areas with wind turbines designed

and constructed to test their functionality and performance. Bhutta et al. [1] reviewed various VAWT configurations, weighing their pros and cons, design techniques used for designing VAWT and their result. Howell et al. [12] completed a similar experiment and documented the behavior of the VAWT with different wind speed velocity, tip-speed ratio, and solidity. Elkhoury et al. [7] performed a combined experimental and analytical VAWT study with a variable pitch design using a wind tunnel. They documented the effects of wind speeds, airfoil shape, and strut mechanisms on the turbine's performance, like what this experiment encompasses. Roy et al. [27] discussed the importance of renewable energy sources, particularly wind energy, and the potential of offshore installations. They also highlighted the limitations of existing vertical-axis wind turbine designs and the need for improved performance for offshore applications. Kumar et al. [14] summarized the development of Darreius turbine technology and their past failures. Rassoulinejad-Mousavi et al. [26] studied a hybrid vertical axis wind turbine (HWT) experimentally, combining a Savonius wind turbine (WT) with a horizontal rotor WT. Ragni et al. [23] presented an experimental investigation of a new airfoil design for lift-driven VAWT and show that the new airfoil design outperformed the NACA designs in terms of lift and drag coefficients. Battisti et al. [3] comprehensively analyzed different blade architectures on small VAWT performance. They discussed the impact of blade number, airfoil camber line, and blade inclination on power and thrust characteristics. Their research objective was to analyze and document the behavior of different blades with a micro form factor for a VAWT, and the effects of blade parameters on lift and drag coefficient. Hammed et al. [11] presented a concept for the design of a straight symmetrical blade for a small-scale vertical axis wind turbine using beam theories for analytical modeling and the commercial software ANSYS 11.0 for numerical modeling. Rajpar et al. [25], in the paper, review the installation position and orientation of the deflectors, and the potential effect, of increasing the power output. The study found that VAWTs are good for working under variable wind speeds and easy installation. However, on the downside, VAWTs have poor self-starting performance, low initial torque, and lower power outputs.

A review of research literature reveals that small-scale portable vertical-axis wind turbines (VAWTs) can offer a compact solution for mobile power generation applications [16, 22, 24]. Although horizontal axis wind turbines remain the predominant industry and academic focus, Savonius-type turbine design may benefit from aerodynamic efficiency improvements through blade shape analytical modeling and optimization [2, 19, 20]. Didane et al. [5] provides a comprehensive overview of VAWTs improvements in terms of aerodynamic modeling, blade configurations, and optimization methods with an extensive literature review. Research aimed to refine blade and rotor geometries, as well as system configurations, for modest power generation has been competed by Ganesh et al. [9] and Gu et al. [10]. Tzen [28] investigated the use of small wind turbines for both off-grid and on-grid energy generation in remote areas. In totality, these studies demonstrate the feasibility and need for additional work on portable omni-directional wind capture VAWT solutions in low-speed wind conditions to charge personal communication devices in a reliable and cost-effective manner [15]. The current research project addresses the aerodynamic optimization of blade geometries and system configuration to enhance the performance of compact wind energy machines to aid the global hiking and backpacking sector.

Micro wind turbines have a small rotor diameter (<1m) and are used for low-power applications. Research work in this area is limited in terms of the size numerically studied. Little evidence exists regarding the effect of blade parameters on the lift and drag co-efficient for a VAWT of this form factor. In this paper, a total of eight blade profiles were examined to perform this numerical study and fulfill the abovementioned purpose. These blades primarily account for the effects of lift and drag coefficient blade parameters. Simulations were run in two commercial packages, COMSOL™ and Qblade™. The rest of the article is organized as follows: Section 3 discusses the blade selection process and blade optimization to yield maximized results. The numerical study in both software packages has been discussed in Section 4. The analytical results of the numerical study are discussed in Section 5, followed by the conclusion in Section 6.

3 WIND TURBINE DESIGN

Tabulated lift and drag coefficients data are required to conduct blade element-based aerodynamic rotor performance simulations. The lift coefficient measures the force generated by the airfoil perpendicular to the flow direction. In contrast, the drag coefficient measures the force generated by the airfoil parallel to the flow direction. These lift and drag coefficients are obtained over a range of angles of attacks (AoA) denoted by alpha XFOIL® [21, 6], supplies these coefficients, and can compute two-dimensional flow around these surfaces by combining a fully coupled viscous/inviscid flow with a high order panel method [17]. XLFR5 [4], an XFOIL® GUI, designs or imports airfoil geometries. The software package Qblade is used to design a wind turbine that features multiple blades. Some modules include a turbine optimization module, a cost of energy calculation module, and a blade dynamics module.

The Qblade algorithm simulates a single-blade profile up to the flow separation regime, which reaches an AoA of 20^0. However, the successful application of this algorithm is highly subjective to the blade profile. The XFOIL® algorithm can estimate the lift and drag coefficients over a range of AoA until stall angles of the given airfoil geometry. These coefficients are plotted vs. AoA as polar graphs. For the XFOIL numerical results to be used in a Blade Element Momentum (BEM) or Double Multiple Streamtube (DMS) methods, the lift and drag polar must be extrapolated to angles far beyond the stall angles. This extrapolation is achieved by assuming that an airfoil at high angles of attack behaves like a flat plate with a sharp leading edge. The post-stall extrapolation model proposed by Montgomerie [18] and Viterna-Corrigan [30] can be applied.

3.1 Simulation Algorithm Theory

The Qblade consideration of a VAWT uses both the BEM and DMS methods. The BEM theory utilizes a uniform, steady state inflow for the two-dimensional blade section of the rotor. The local blade forces are then calculated by integrating the lift and drag forces over each blade element. The DMS method estimates the local blade forces and accounts for the global flow field. The turbine is modeled as a rotor with two discs, where one of the rotors is upstream and the other is downstream, as shown in Figure 2. The rotor blade is discretized into user-specified elements in 5^0 incremental steps to create a circular path. An assumption is made that the velocity decreases by one-half as the flow passes each disc. The rotor extracts kinetic energy from the incoming wind at the upstream and the downstream disc. The global flow field is then calculated using the DMS. The rotor loads and performance are calculated using BEM's local blade forces and DMS's global flow field. The three-dimensional effects are not accounted for in this, but the impact on rotor loads and performance is included in the simulations utilizing a semi-empirical correction. The velocity at the upstream rotor disc, V_{up}, downstream rotor disc, V_{down} and at the equilibrium between the two discs, V_{eq}, are given as follows, and a more detailed derivation of these equations can be found in [4].

$$V_{up} = u_{up} * V_0 \tag{1}$$

$$V_{down} = u_{down}(2u_{up} - 1) * V_0 \tag{2}$$

$$V_{eq} = (2u_{up} - 1) * V_0 \tag{3}$$

where V_0 is the inflow wind velocity, while u_{up} and u_{down} are the upstream and downstream interference factors.

The values for normal and thrust coefficients, C_N and C_T, can be evaluated by using the lift and drag values C_l and C_d from the UIUC airfoil database.

$$C_N = C_l \cos\alpha + C_d \cos\alpha \tag{4}$$

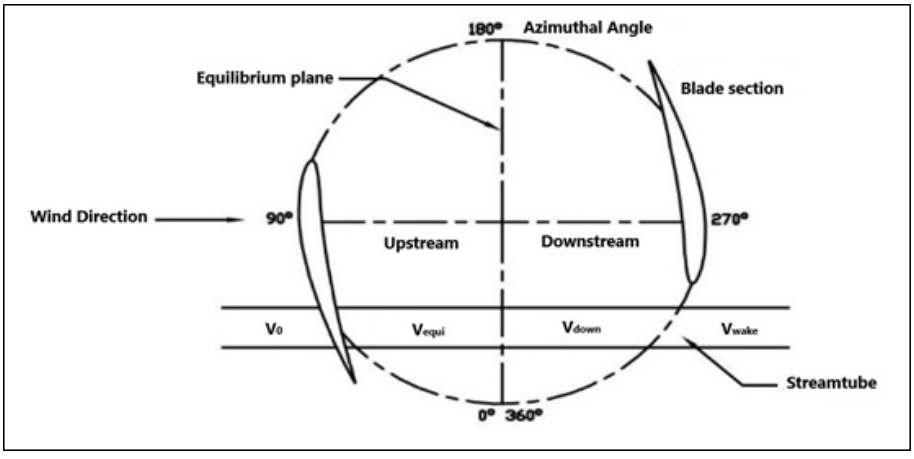

Figure 2: Double multiple stream tube model for wind turbine blades

$$C_T = C_l \cos\alpha - C_d \cos\alpha \tag{5}$$

where α is the angle of attack.

These normal and thrust coefficient values are used to estimate the upstream interference factor, which is derived from Blade Element Theory and the momentum equation over each stream tube so that

$$u_{up} = \frac{8\pi^2 r}{Nc}\left(\int_{-\pi/2}^{\pi/2} \frac{1}{|\cos\theta|}\left[C_N \cos\theta - C_T \frac{\sin\theta}{\cos\delta}\right]\left(\frac{W^2}{V_{up}^2}\right) d\theta\right)^{-1} \tag{6}$$

where θ is the azimuthal angle, δ is the angle between the turbine axis and the blade normal, r is the rotor radius, N is the number of blades in the rotor, and c is the chord length.

To calculate the value for the thrust and normal coefficients, we need the angle of attack, α, which is given by

$$\alpha = sin^{-1}\left[\left(\cos\theta\cos\delta\cos\alpha_0 - \left(\frac{r\omega}{V_{up}} - \sin\theta\right)\sin\alpha_0\right)\frac{V_{up}}{W}\right] \tag{7}$$

where α_0 is the blade twist angle, ω is the angular velocity of the rotor, and W is the relative velocity and can be calculated as

$$W = V_{up}\sqrt{\left(\frac{r\omega}{V_{up}} - \sin\theta\right)^2 + \cos^2\theta\cos^2\delta} \tag{8}$$

To estimate the value for V_{up}, we assume $u_{up} = 1$, and then, using that value for V_{up}, we estimate the new value for u_{up} until we reach convergence for these values. The downstream interference factor is estimated using the same process and equation as u_{up} instead of V_{down} and integrating from $\pi/2$ to $3\pi/2$. Once the interference factors are estimated, the blade forces and performance can be estimated by averaging over one revolution.

3.2 Blade Profile Design

Designing the blade profile for a VAWT involves optimizing the aerodynamic performance to ensure efficient energy capture while considering structural integrity and the turbine's operational environment. There are quite a few aspects of designing the blade for VAWT as listed below [11, 1].

- Airfoil Selection:
  - Choose airfoil shapes that balance lift and drag for optimal performance.
  - The airfoil should be designed to avoid flow separation and turbulence, especially at high wind speeds.
- Blade Angle of Attack:
  - The blade's angle of attack should be optimized to capture the maximum amount of wind energy without causing excessive drag.
- Twist and Curvature:
  - Incorporate blade twist to maintain an effective angle of attack along the entire length of the blade as the wind velocity changes.
  - A curved blade profile can improve the aerodynamic efficiency, providing smoother airflow over the surface.
- Length-to-Width Ratio:
  - Optimize the aspect ratio (blade length vs. width) for the intended wind speed range.
  - A higher aspect ratio may improve efficiency but can increase structural challenges.
- Camber and Thickness Distribution:
  - Design the blade with an appropriate camber to balance lift and drag.
  - Ensure the thickness of the airfoil varies along the length of the blade to maintain structural integrity and aerodynamic efficiency.
- Blade Tip Shape:
  - Consider designing the blade tips with a tapered or rounded shape to reduce vortex drag and tip losses.
  - Blade tip designs like winglets or elliptical shapes can improve efficiency by reducing turbulent flow at the tips.
- Sweep and Cord Length Variation:
  - Design the blade profile to vary the chord length (width of the blade at any given point) along its length to optimize performance at different wind speeds.
  - Blades may be wider near the base (hub) and narrower toward the tip to balance structural strength and aerodynamics.
- Flow Separation and Stall Resistance:
  - The profile should be resistant to flow separation to prevent performance loss, particularly at higher angles of attack.

– Incorporate features like surface roughness or vortex generators to delay stall and improve power generation at lower wind speeds.

Simulations are conducted under consistent conditions for an accurate comparison of the performance of different blade designs. The simulations make the following assumptions to maintain consistency across the software packages. The flow is steady and two-dimensional. The flow around a wind turbine blade is unsteady and three-dimensional. The simulations do not account for the effects of blade root stall or tip vortex cavitation. The results of this study can provide valuable insights into the relationship between airfoil geometry, blade parameters, and aerodynamic performance. Further, the results allow for comparison of the lift and drag coefficients of the eight-blade designs to determine which airfoil geometry and blade parameters produce the best aerodynamic performance (refer to Table 1). This information can then be used to design more efficient wind turbines and reduce the cost of wind energy.

The CFD software requires airfoil parameter data to run simulations, which is used for testing. This data is imported into the CFD software packages in two ways. It can be obtained in Qblade by using the airfoil generator module, which requires the NACA airfoil numbers (NACA 'XXXX') to generate the airfoil. Another method is to import the coordinate data file from the UIUC database into Qblade. The latter's advantage is that parameter changes, such as pitch, camber radius, etc., can be made and then imported into Qblade, which are directly reflected in the GUI of Qblade. The GUI displays the imported airfoils, as shown in Figure 3. The airfoil geometry imported into COMSOL Multiphysics works differently than in Qblade. Once the necessary parameter changes are made in the airfoil plotter, the plotted airfoil can be imported directly into COMSOL Multiphysics, and the CFD analysis can be performed. To compare the results, the operating conditions are kept the same for the analyses performed in Qblade and COMSOL Multiphysics. Blades 6 and 8 in Table 1 can only be run in COMSOL as Qblade has limitations that prevent non-standard geometries from being imported into the software package.

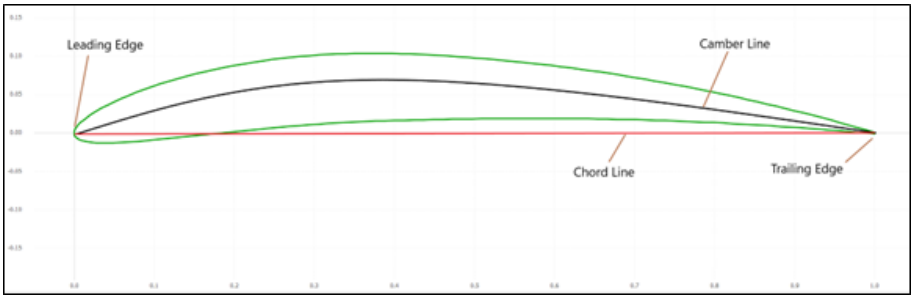

Figure 3: NACA 6409 9% airfoil imported in CFD software with the airfoil parameters

3.3 Blade Optimization

Blade parameters, such as chord length, camber radius, pitch angle, and thickness, play a significant role in determining the aerodynamic performance of wind turbine blades. Changes in these parameters can influence the lift and drag coefficients, which in turn affect the power generation capabilities of the turbine to validate the results. Figure 3 shows the blade parameters for a NACA 6409 9% imported in CFD software. Chord length, the distance from the leading edge to the airfoil's trailing edge, is a crucial parameter affecting the blade's lift and drag characteristics. Generally, increasing the chord length tends to increase both lift and drag. However, the rate of increase in drag is typically higher than the increase in lift, leading to a decreased lift-to-drag ratio. This means that while a longer chord length may generate more lift, it also produces more drag, potentially reducing the turbine's overall efficiency. Camber radius, the curvature of the airfoil's upper

Table 1: List of blade profile designs where (H) are blades for HAWT and (V) are blades for VAWT

Blade No.	Description	Blade Profile
1	NACA 6409 9% Camber 120mm (H)	
2	NACA 6409 9% Camber 150mm (H)	
3	NACA 6409 9% Camber 300mm (H)	
4	NACA 6409 9% Camber 450mm (H)	
5	Urginsky Rotor Blade (V)	
6	Bergey BW-3 (H)	
7	FX 77-W-121 (H)	
8	Savonius - Bucket (V)	

surface, significantly impacts the blade's lift and drag performance. A higher camber radius generally leads to increased lift and a delayed stall point. However, it also results in increased drag at higher angles of attack. Pitch angle, the angle between the airfoil's chord line and the blade's plane of rotation, affects the blade's angle of attack relative to the incoming wind flow. Adjusting the pitch angle can optimize lift and drag characteristics for different operating conditions. Airfoil thickness, the distance from the upper surface to the lower surface of the airfoil at any point along the chord, also influences lift and drag. Generally, thicker airfoils tend to generate more lift at lower angles of attack, but experience increased drag at higher angles of attack.

The effects of camber radius on lift and drag coefficients are investigated in this experimental study using four different NACA 6409 9% airfoils with varying camber radii: 120, 150, 300, and 450 mm. Figure 4 shows the difference between the various NACA blades selected for this study. Each airfoil's lift and drag coefficients were measured at different angles of attack and plotted vs. AoA to determine their aerodynamic performance. Computational fluid dynamics (CFD) simulations were performed using COMSOL Multiphysics to analyze the aerodynamic behavior of the airfoils further. CFD simulations provide detailed insights into the flow patterns around the airfoils, allowing for a more comprehensive understanding of their lift and drag characteristics. These results were then used to validate the performance of the airfoils and identify the optimal camber radius for achieving maximum power generation. The findings of this study can be applied to optimize the design of wind turbine blades for improved efficiency and power output. Understanding the influence of blade parameters on lift and drag coefficients is essential for optimizing the aerodynamic performance of wind turbine blades. By carefully considering the effects of chord length, camber radius, pitch angle, and thickness, engineers can design blades that generate more lift with less drag, leading to increased power generation and improved wind turbine efficiency.

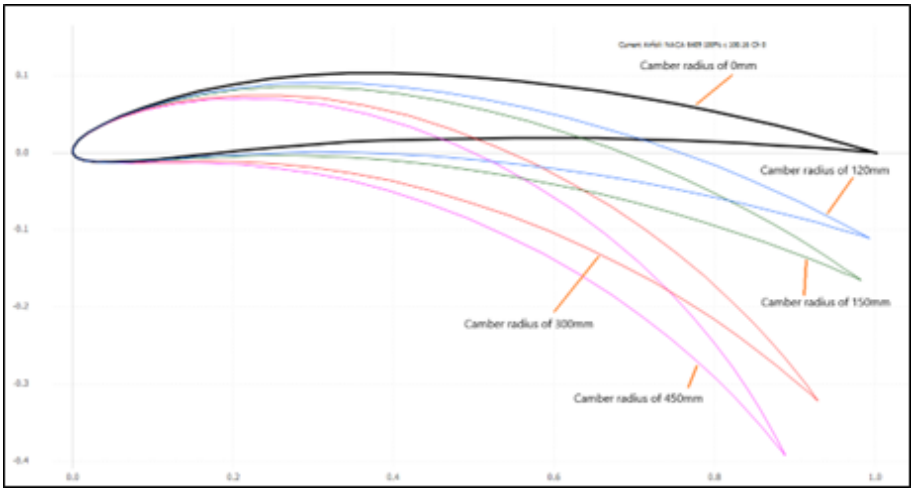

Figure 4: NACA 6409 9% properties for different camber radii

4 Case Study - Micro Wind Turbine

Simulations for the turbine rotors were completed in Qblade and COMSOL Multiphysics. The initial conditions for the simulations are the same, with minor differences attributed to the programming of the CFD software. In Qblade, once the airfoil geometry is imported, the airfoil analysis module allows the run of lift and drag simulations from a start to a finish angle with a user-defined step value. Parameters such as Reynold's number, Mach number, N-Crit, forced top transition, and forced bottom transition can be defined in this module. Figure

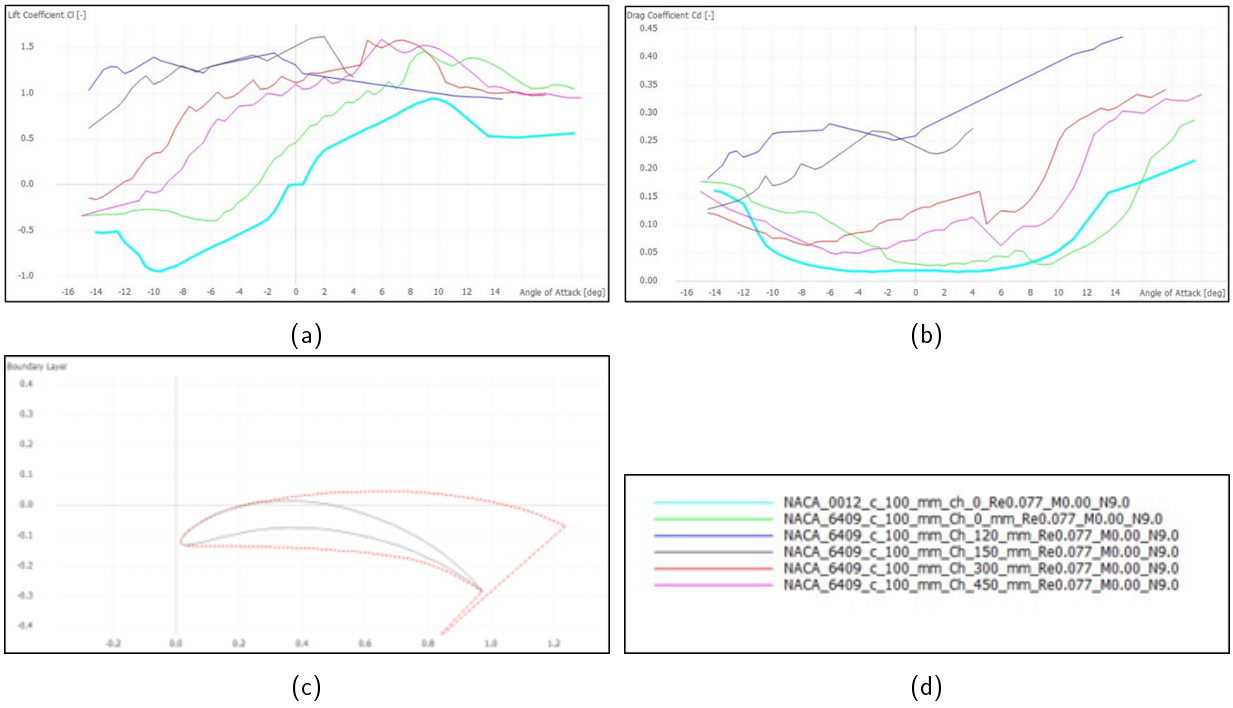

Figure 5: Lift (5a) and drag (5b) coefficient polar plots in Qblade with the corresponding boundary layer (5c), and legend (5d, for six NACA blade profiles (Blades No. 1-4).

5 shows the lift, drag and boundary layer plots derived from the airfoil analysis module. The wind flow velocity cannot be defined in the software package; consequentially, the Reynolds number *Re*, will apply as follows

$$Re = \frac{\rho u L}{\mu} \tag{9}$$

where ρ is the density of the fluid, u is the flow speed, L is the characteristic length, and μ is the dynamic fluid viscosity.

The CFD software packages perform the analysis differently with different methodologies for defining parameters. Qblade runs the simulations based on the parameters set for a specific airfoil. For this study, we set the Reynolds number to 77,000, corresponding to a wind flow speed of 11.5 m/s of the fan. The rest of the parameters in the airfoil analysis module are kept the same as the system default. The airfoil analysis module estimates a chosen airfoil's lift and drag coefficients and runs simulations for all the specified angles. It is important to note that Qblade only runs simulations for airfoils between the specified angles until a flow separation regime is achieved for that airfoil. This could be, for example, 1^0 to 5^0 for one airfoil and $-16^0 - 20^0$ for other airfoils. Since Qblade stops its simulation runs at the flow separation regime, extrapolation is required for a 360^0 revolution of the rotor (see Section 3). Figure 6 shows the extrapolation for a NACA 0012 airfoil. COMSOL Multiphysics uses a different methodology. It is used to estimate the lift and drag of a selected airfoil. Laminar 2D steady-state flow is used to study the physics of the airfoil. A rectangular area with a length of 762 mm and a width of 215.9 mm, which corresponds to the top view of the wind tunnel, is defined. The airfoil geometry is then imported into this rectangular area, as shown in Figure 7. The inlet wind velocity

is set to 11.5 m/s. Parametric sweep is enabled for the AoA, which allows the software to run simulations for a range of AoA.

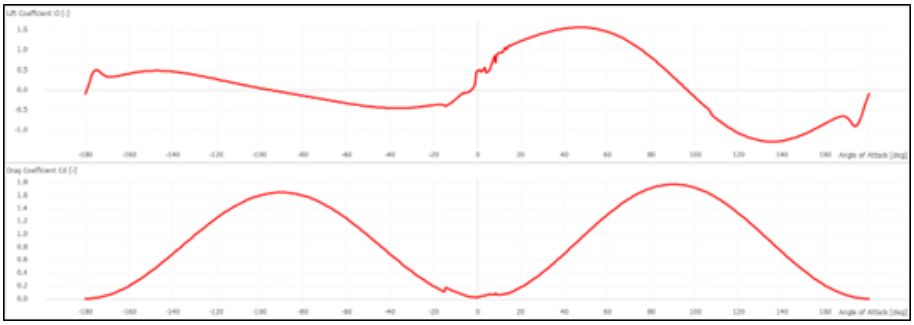

Figure 6: Lift (top) and drag (bottom) coefficient extrapolation polar graphs in Qblade for a FX 77-W-121 blade profile.

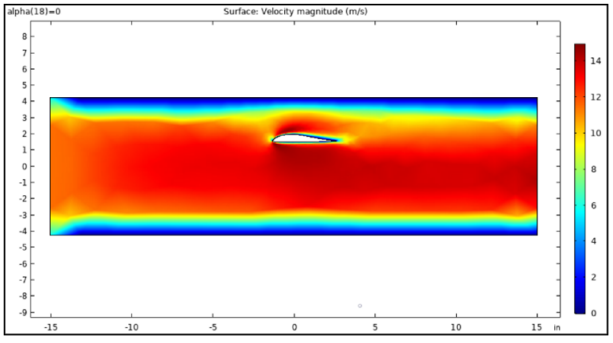

Figure 7: Velocity plot for an FX-77-121 blade profile imported in COMSOL with a magnitude ranging from 0 to 14 m/s

5 Analytical Results

The CFD simulations were conducted for all eight blade profiles to analyze their aerodynamic performance. The simulations were performed using Qblade (Method 1) and COMSOL Multiphysics (Method 2), providing a comprehensive assessment of the lift and drag characteristics of the airfoils. The lift and drag coefficients, crucial parameters in determining the aerodynamic efficiency of an airfoil, were calculated for each blade design at various angles of attack. The lift and drag coefficients for all eight blade designs are presented in Table 2. The table shows how each airfoil's lift and drag coefficients vary with AoA. These values provide valuable insights into the aerodynamic performance of the blades under different operating conditions. Figure 8 visually illustrates the lift and drag coefficients of the eight-blade designs plotted against AoA. The plots demonstrate the relationship between the blade's angle of attack and its aerodynamic performance. Due to computational limitations, analytical results for blades 5 and 8 were only obtained using Method 2.

Blades 1-4 belong to the same family but have different camber radii, which show a general trend of decreasing lift and drag coefficient with increasing camber radii. Blades 1 and 2 have a similar profile, having camber radii of 120 and 150mm, respectively. The lift coefficients computed in COMSOL for both these blades

Table 2: Analytical data for various blade designs

Blade No.	Description	Max Analytical Lift Coefficient C_L				Max Analytical Lift Coefficient C_D			
		Angle of Attack, α (deg)	Qblade	Angle of Attack, α (deg)	COMSOL	Angle of Attack, α (deg)	Qblade	Angle of Attack, α (deg)	COMSOL
1	NACA 6409 9% Camber 120mm (H)	-6	1.44	14.5	3.47	11	0.44	14.5	1.31
2	NACA 6409 9% Camber 150mm (H)	2	1.61	4	2.22	-3	0.27	-3	0.7
3	NACA 6409 9% Camber 300mm (H)	7	1.58	16.5	2.75	1	0.43	4.5	0.44
4	NACA 6409 9% Camber 450mm (H)	6	1.59	20	2.52	17.5	0.33	1	0.28
5	Urginsky Rotor Blade (V)	DNR*	DNR*	-15	-2.60	DNR*	DNR*	0.5	2.91
6	Bergey BW-3 (H)	9	1.4	20	2	20	0.31	-1	0.16
7	FX 77-W-121 (H)	13.5	1.005	13.5	1.89	-15	0.17	-1	0.167
8	Savonius-Bucket (V)	DNR*	DNR*	-11.5	-0.075	DNR*	DNR*	-7.5	0.65

*DNR - Does Not Run

see the same trend, viz., they both increase with the increase in the AoA from -15^0 to 15^0, although blade 1 has a slightly larger CL compared to blade 2. This can be seen in Figure 8 (a) and (b). In Method 1, the lift coefficients for blades 1 and 2 show a similar trend with an increase in the CL up to 1.4 and 1.6, respectively, at an AoA of 0^0, which decreases as the AoA increases. The drag coefficient for blades 1 and 2 exhibit the same trend in both software packages. The values for CD in both methods differ by a factor of 3, and the values are almost double between the two blades. Blades 3 and 4 observe a similar trend for both CL and CD in both software packages. The values for both coefficients are close, as shown in Figures 8 (c) and (d). The maximum analytical lift coefficient for blades 3 and 4 in Method 1 is at 7^0 and 6^0, respectively, which is not the case for the maximum drag coefficient for these blades. A general trend is observed in blades 1-4, especially for lift and drag coefficients obtained in Method 2. As the camber radius increases, the maximum lift and drag coefficient values decrease, as seen in Table 2.

Blades 5-6 belong to different families and have varying camber radii. Blade 5 has a maximum lift coefficient of -2.6 and a maximum drag coefficient of 2.91 at -15^0 and 0.5^0 respectively. A negative value for the lift coefficient means the blade rotates in the opposite direction (anti-clockwise). The lift and drag values could not be obtained in Method 1. Blades 6 and 7 are designed for low Reynolds numbers, best suited for this study. Once again, we see a similar trend in all values for both the blades in both the software packages. The maximum analytical values for both these blades are different and occur at different AoAs except for the maximum drag coefficient obtained in COMSOL, which is the same for both these blades and occurs at the same AoA. Blade 8 is a Savonius - bucket-type blade. Like blade five, this also could not be run in Method 1. The maximum values for lift and drag coefficients were obtained in COMSOL. The maximum lift co-efficient is -0.075 at an AoA of -11.5^0, and the maximum drag co-efficient is 0.65 obtained at an AoA of -7.5^0.

The CFD simulations for these blades were computationally more demanding due to their complex geometries. A comparison of CFD simulation results obtained from Method 1 and Method 2 revealed good agreement between the two software packages. The lift and drag coefficients calculated using both methods showed similar trends and values, demonstrating the simulation methodology's validity. The simulation results provide valuable information for optimizing the design of wind turbine blades. By analyzing different airfoil profiles' lift and drag characteristics, engineers can identify the most efficient blade configurations for maximizing power generation and improving wind turbine performance. In conclusion, the CFD simulations conducted in this study provide a comprehensive understanding of the aerodynamic performance of eight different blade profiles. The lift and drag coefficients calculated for each blade design at various angles of attack provide valuable insights into their suitability for wind turbine applications. The comparison of results from Method 1 and Method 2 further validates the accuracy of the simulation methodology. These findings can be utilized to optimize blade design and enhance the efficiency of wind turbines.

6 CONCLUSIONS

Vertical axis wind turbines have gained increasing attention as a promising alternative to horizontal axis wind turbines for harnessing wind energy. VAWTs offer several advantages over HAWTs, including their ability to operate at low wind speeds and their adaptability to complex urban environments. However, the miniaturization of VAWTs has been relatively unexplored, with limited research focusing on the design and optimization of small-scale VAWTs. While larger form factors generally lead to higher power output, they also increase structural requirements and manufacturing costs. Miniaturizing VAWTs necessitates reducing form factor, which poses challenges in maintaining aerodynamic efficiency. Selecting appropriate blade profiles is crucial for maximizing aerodynamic performance in small-scale VAWTs. Conventional blade profiles designed for larger VAWTs may not be optimal for miniaturized turbines due to their different aerodynamic characteristics at lower wind speeds and higher blade tip speeds. Researchers are exploring various blade profiles specifically designed for small-scale VAWTs, considering factors such as reduced drag, enhanced lift at low angles of attack, and improved stall behavior. In this study, eight different blade profiles for miniature VAWTs were analyzed in

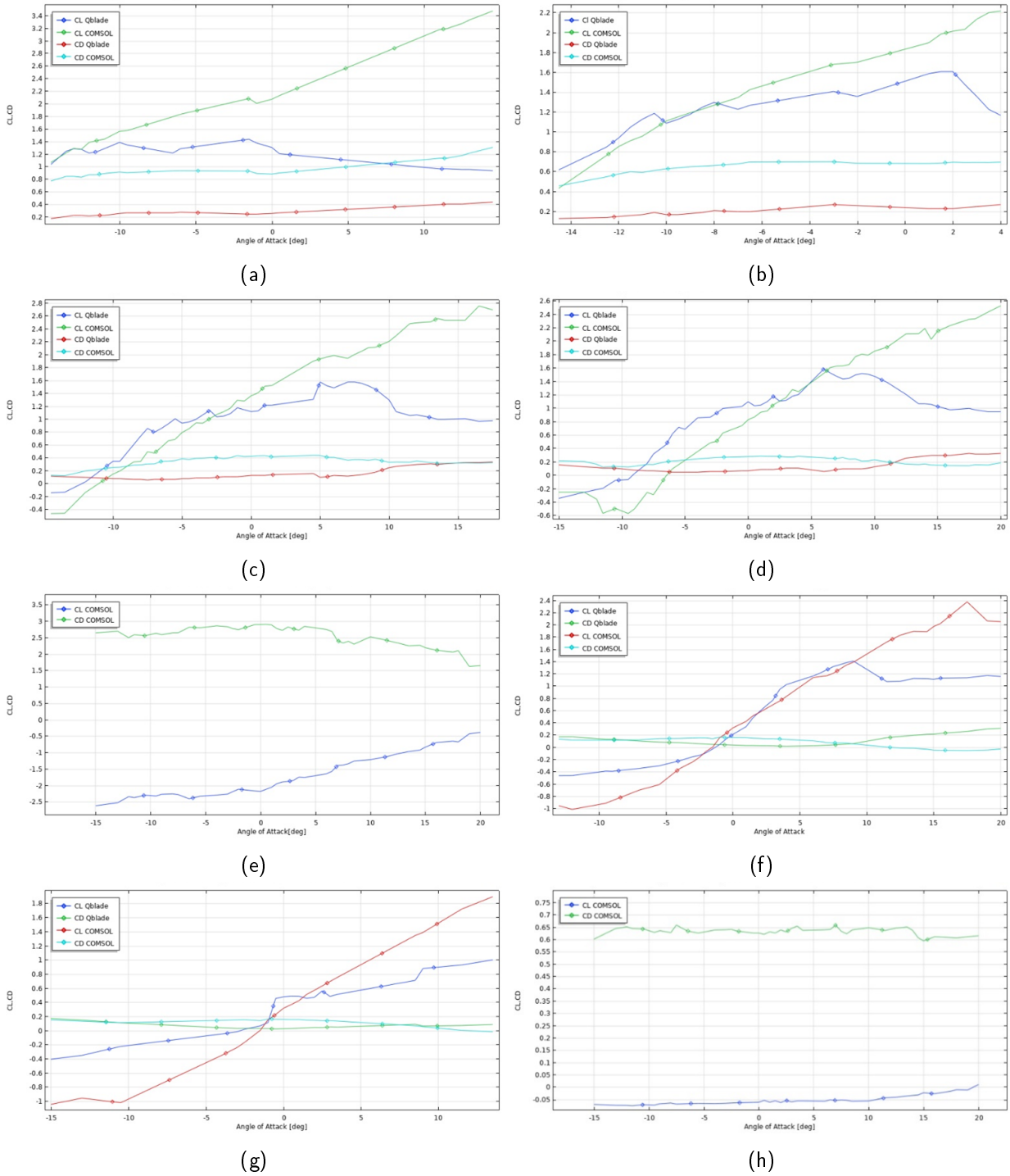

Figure 8: Lift and Drag coefficients for NACA 6409 9% with a camber of (a) 120mm, (b) 150mm, (c) 300mm, (d) 450mm, and (e) Urginsky rotor, (f) Bergey BW-3, (g) FX-77-121, and (h) Savonius - bucket blade vs. Angle of Attack [deg]

two software packages, Qblade and COMSOL. As expected, blades with a curved profile have an increased lift and drag coefficient, which corresponds to increased lift and drag forces. Qblade has limitations due to the software's focus on larger-scale applications. Additionally, the software's library of blade profiles may not include those specifically designed for miniaturized turbines. On the other hand, COMSOL enables direct importing of blade profiles and can accommodate miniature designs. Feasible designs were identified through performance measures, and a multibladed VAWT will be fabricated for laboratory testing in the next phase of this research project, as shown in Figure 9. Research into small-scale VAWTs is crucial for overcoming the challenges associated with miniaturization and developing efficient and cost-effective turbines for these applications.

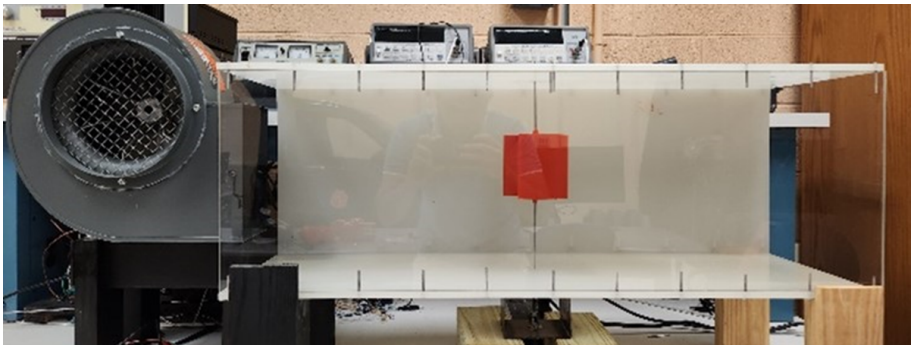

Figure 9: Experimental set-up with a small-scale wind tunnel and a variable-speed electric blower

Satchit Ramnath, http://orcid.org/0000-0002-2509-0626

APPENDIX - Nomenclature List

Abbreviations

AoA	Angle of Attack
BEM	Blade Element Theory
CFD	Computational Fluid Dynamics
DMS	Double Multiple Streamtube
GUI	Graphical User Interface
HAWT	Horizontal Axis Wind Turbine
NACA	National Advisory Committee for Aeronautics
VAWT	Vertical Axis Wind Turbine

Symbols

c	Chord length (m)
C_N	Thrust coefficient
C_T	Normal coefficient
C_l	Lift coefficient
C_d	Drag coefficient
L	Characteristic length (m)
N	Number of blades
r	Radius of rotor (m)
Re	Reynold's number
u	Flow speed (m/s)
u_{up}	Upstream interference factor
u_{down}	Downstream interference factor
V_{up}	Upstream rotor disc velocity (m/s)
V_{down}	Downstream rotor disc velocity (m/s)
V_{eq}	Velocity at equilibrium between the two discs (m/s)
V_0	Inflow wind velocity (m/s)
W	Relative velocity (m/s)
α	Angle of attack (rad)
α_0	Blade twist angle (rads)
δ	Angle between turbine axis and blade normal (rad)
θ	Azimuthal angle (rads)
μ	Kinematic viscosity (m2/s)
ρ	Density of fluid (kg/m3)
ω	Angular velocity (rads/s)

REFERENCES

[1] Aslam Bhutta, M.M.; Hayat, N.; Farooq, A.U.; Ali, Z.; Jamil, S.R.; Hussain, Z.: Vertical axis wind turbine - A review of various configurations and design techniques. Renewable and Sustainable Energy Reviews, 16(4), 1926–1939, 2012. ISSN 13640321. http://doi.org/10.1016/j.rser.2011.12.004.

[2] Avallone, E.; Palota, P.; Mioralli, P.; Natividade, P.; Antonio, J.; Ferreira, d.; Verdério, S.: Savonius micro wind turbine: A theoretical analysis. Facta universitatis - series: Electronics and Energetics, 36(2), 227–238, 2023. ISSN 0353-3670. http://doi.org/10.2298/FUEE2302227A.

[3] Battisti, L.; Brighenti, A.; Benini, E.; Castelli, M.R.: Analysis of Different Blade Architectures on small VAWT Performance. Journal of Physics: Conference Series, 753, 062009, 2016. ISSN 1742-6588. http://doi.org/10.1088/1742-6596/753/6/062009.

[4] Deperrois, A.: XFLR5 Analysis of Foils and Wings Operating at Low Reynolds Numbers. Ph.D. thesis, Purdue University, West Lafayette, Indiana, 2009.

[5] Didane, D.H.; Behery, M.R.; Al-Ghriybah, M.; Manshoor, B.: Recent Progress in Design and Performance

Analysis of Vertical-Axis Wind Turbines - A Comprehensive Review. Processes, 12(6), 1094, 2024. ISSN 2227-9717. http://doi.org/10.3390/pr12061094.

[6] Drela, M.: XFOIL: An Analysis and Design System for Low Reynolds Number Airfoils. 1–12, 1989. http://doi.org/10.1007/978-3-642-84010-4{_}1.

[7] Elkhoury, M.; Kiwata, T.; Aoun, E.: Experimental and numerical investigation of a three-dimensional vertical-axis wind turbine with variable-pitch. Journal of Wind Engineering and Industrial Aerodynamics, 139, 111–123, 2015. ISSN 01676105. http://doi.org/10.1016/j.jweia.2015.01.004.

[8] ExxonMobil: Energy Demand: Three Drivers, 2024. https://corporate.exxonmobil.com/sustainability-and-reports/global-outlook/energy-demand-drivers.

[9] Ganesh, A.S.; Babu, A.J.; Sai, B.H.; Prasad, B.; Madhuri, C.: Design and Analysis of Vertical Axis Wind Turbine Blades for Mini Power Generation. International Journal of Scientific Research and Engineering Development, 8(2), 2025.

[10] GU, Y.; KAMEL, E.; TSITRON, I.; AGINSKIY, M.: DESIGN AND PERFORMANCE STUDY OF A UNIQUE MODULAR VERTICAL AXIS WIND TURBINE. 93–100, 2021. http://doi.org/10.2495/ESUS210091.

[11] Hameed, M.S.; Afaq, S.K.: Design and analysis of a straight bladed vertical axis wind turbine blade using analytical and numerical techniques. Ocean Engineering, 57, 248–255, 2013. ISSN 00298018. http://doi.org/10.1016/j.oceaneng.2012.09.007.

[12] Howell, R.; Qin, N.; Edwards, J.; Durrani, N.: Wind tunnel and numerical study of a small vertical axis wind turbine. Renewable Energy, 35(2), 412–422, 2010. ISSN 09601481. http://doi.org/10.1016/j.renene.2009.07.025.

[13] Khudri Johari, M.; Azim A Jalil, M.; Faizal Mohd Shariff, M.: Comparison of horizontal axis wind turbine (HAWT) and vertical axis wind turbine (VAWT). International Journal of Engineering & Technology, 7(4.13), 74–80, 2018. ISSN 2227-524X. http://doi.org/10.14419/ijet.v7i4.13.21333.

[14] Kumar, P.M.; Rashmitha, S.R.; Srikanth, N.; Lim, T.C.: Wind Tunnel Validation of Double Multiple Streamtube Model for Vertical Axis Wind Turbine. Smart Grid and Renewable Energy, 08(12), 412–424, 2017. ISSN 2151-481X. http://doi.org/10.4236/sgre.2017.812027.

[15] Lee, K.Y.; Cruden, A.; Ng, J.H.; Wong, K.H.: Variable designs of vertical axis wind turbines - a review. Frontiers in Energy Research, 12, 2024. ISSN 2296-598X. http://doi.org/10.3389/fenrg.2024.1437800.

[16] Mangate, L.; Jadhav, D.; Gavade, V.; Deshmukh, L.; Gore, A.; Gangde, G.; Jadhav, A.: Harnessing Wind Power for On-the-Go Device Charging: The Portable Mobile Charger Revolution. In 2024 International BIT Conference (BITCON), 1–5. IEEE, 2024. ISBN 979-8-3315-1839-4. http://doi.org/10.1109/BITCON63716.2024.10985636.

[17] Marten, D.; Wendler, J.; Pechlivanoglou, G.; Nayeri, C.N.; Paschereit, C.O.: Development and Application of a Simulation Tool for Vertical and Horizontal Axis Wind Turbines. In Volume 8: Supercritical CO2 Power Cycles; Wind Energy; Honors and Awards. American Society of Mechanical Engineers, 2013. ISBN 978-0-7918-5529-4. http://doi.org/10.1115/GT2013-94979.

[18] Montgomerie, B.: Methods for Root Effects, Tip Effects and Extending The Angle of Attack Range to +-100°, with Application to Aerodynamics for Blades on Wind Turbines and Propellers. Tech. rep., Swedish Defense Research Agency, Stockholm, 2004.

[19] Nachaiyaphum, K.; Photong, C.: An electric power generation improvement for small Savonius wind turbines under low-speed wind. Indonesian Journal of Electrical Engineering and Computer Science, 29(2), 618, 2023. ISSN 2502-4760. http://doi.org/10.11591/ijeecs.v29.i2.pp618-625.

[20] Ouchiha, Z.; Iddou, H.; Legouini, T.; Hamrit, A.: Evaluation of the Performance of a Savonius Micro Wind Turbine. 741–749, 2025. http://doi.org/10.1007/978-3-031-80301-7{_}77.

[21] Paraschivoiu, I.: Wind Turbine Design: With Emphasis on Darrieus Concept, 2002. ISBN 9782553009310.

[22] Pawar, Y.G.; Katkade, O.V.; Ahire, V.H.: Small Scale Vertical Axis Portable Wind Turbine for Charging Electronic Gadgets. International Journal of Engineering Research & Technology, 4(2), 2015.

[23] Ragni, D.; Ferreira, C.S.; Correale, G.: Experimental investigation of an optimized airfoil for vertical-axis wind turbines. Wind Energy, 18(9), 1629–1643, 2015. ISSN 1095-4244. http://doi.org/10.1002/we.1780.

[24] Rajan, R.; Panchalogaranjan, V.; Aravinthan, V.; Thiruvaran, T.; Shanmugarajah, V.: Low Cost Portable Wind Power Generation For Mobile Charging Applications. In 2018 IEEE International Conference on Information and Automation for Sustainability (ICIAfS), 1–5. IEEE, 2018. ISBN 978-1-5386-9418-3. http://doi.org/10.1109/ICIAFS.2018.8913331.

[25] Rajpar, A.H.; Ali, I.; Eladwi, A.E.; Bashir, M.B.A.: Recent Development in the Design of Wind Deflectors for Vertical Axis Wind Turbine: A Review. Energies, 14(16), 5140, 2021. ISSN 1996-1073. http://doi.org/10.3390/en14165140.

[26] Rassoulinejad-Mousavi, S.M.; M. Jamil; M. Layeghi: Experimental study of a combined three bucket H-rotor with savonius wind turbine. World Applied Sciences Journal, 28(2), 205–211, 2013.

[27] Roy, S.; Branger, H.; Luneau, C.; Bourras, D.; Paillard, B.: Design of an Offshore Three-Bladed Vertical Axis Wind Turbine for Wind Tunnel Experiments. In Volume 10: Ocean Renewable Energy. American Society of Mechanical Engineers, 2017. ISBN 978-0-7918-5778-6. http://doi.org/10.1115/OMAE2017-61512.

[28] Tzen, E.: Small wind turbines for on grid and off grid applications. IOP Conference Series: Earth and Environmental Science, 410(1), 012047, 2020. ISSN 1755-1307. http://doi.org/10.1088/1755-1315/410/1/012047.

[29] U.S. Energy Information Administration: World Energy Projection System, Annual Energy Outlook 2023, 2023. https://www.eia.gov/outlooks/ieo/data/pdf/E_gen_E3.gen_r_230822.081459.pdf.

[30] Viterna, L.A.; Janetzke, D.: Theoretical and Experimental Power from Large Horizontal-Axis Wind Turbines, Technical Report N82-33830. Tech. rep., NASA Lewis Research Centre, Cleveland, Ohio, 1982.